

Contents

World Climate Conference-3 (WCC-3)	1
El Niño Outlook (October 2009 – April 2010)	2
JMA's Seasonal Numerical Ensemble Prediction for Winter 2009/2010	4
Cold-season Outlook for Winter 2009/2010 in Japan	5
Summary of the 2009 Asian Summer Monsoon	7
Status of the Antarctic Ozone Hole in 2009	9
Heavy precipitation in the Philippines and India from late September to early October 2009	9

World Climate Conference-3 (WCC-3)

The World Climate Conference-3 (WCC-3) was held in Geneva, Switzerland, from 31 August to 4 September 2009. WCC-3 was organized by the World Meteorological Organization (WMO) in collaboration with the United Nations Educational Scientific and Cultural Organization (UNESCO), the United Nations Environment Programme (UNEP), the Food and Agriculture Organization of the United Nations (FAO), the International Council for Science (ICSU) and other intergovernmental and non-governmental partners. Some 2,000 participants (8 from the Japan Meteorological Agency (JMA)) from 163 countries and 59 international organizations attended the event.

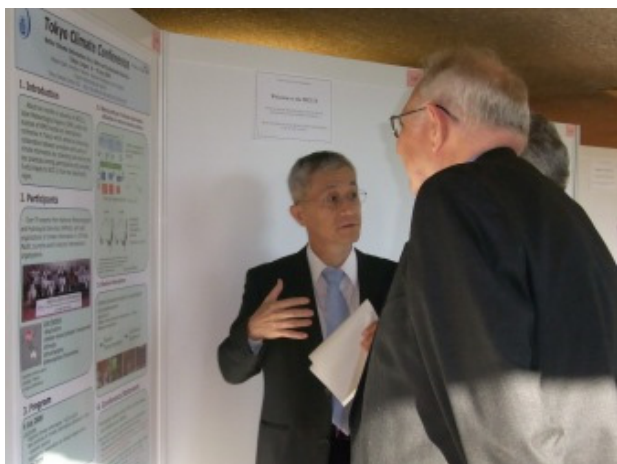
The theme of the Conference was Climate Prediction and Information for Decision Making, and its vision was for an international framework for climate services that

links science-based climate predictions and information with the management of climate-related risks and opportunities in support of adaptation to climate variability and change in both developed and developing countries. The WCC-3 body consisted of expert and high-level segments.

Expert Segment (31 August – 2 September)

Some 200 speakers and 1,500 climate scientists and other experts from climate service providers and user communities reviewed global, sectoral and national needs and capabilities for the provision and application of climate services, and identified the essential elements of a new global framework to be elaborated in a Conference Statement.

At the poster session, Dr. Masaro Saiki, Director-



Dr. Masaro Saiki explains the Tokyo Climate Conference at the poster session.



Dr. Kiyoharu Takano (middle), Director of JMA's Climate Prediction Division, serves as theme leader for the *Regional Climate Information for Risk Management* parallel working session. (Also shown are Dr. Yap Kok Seng, Session Chair and Director-General of the Malaysian Meteorological Department (left) and Dr. Edwin Aldrian of Indonesia's Meteorological Climatological and Geophysical Agency (BMKG) (right).)

General of the Global Environment and Marine Department of JMA, reported on the *Tokyo Climate Conference: Better Climate Information for a Safe and Sustainable Society* held in Tokyo from 6 – 8 July 2009 and organized by JMA ([please refer to TCC News No. 17 for details](#)).

Dr. Kiyoharu Takano, Director of JMA's Climate Prediction Division, served as a theme leader at one of the working parallel sessions titled *Regional Climate Information for Risk Management*. After two presentations of white papers, the session expressed strong support for the strengthening of (1) provider-user partnerships, (2) integrated weather-climate information, (3) regional capacity building, and (4) observation, monitoring and research.

Ms. Kumi Hayashi, Head of JMA's Tokyo Climate Center (TCC), introduced the activities of Regional Climate Centers in Asia (i.e., the China Meteorological Administration's Beijing Climate Center and JMA's TCC) at one of the sessions titled *Implementing Climate Services: Nations and Regions*.

High-level Segment (3 – 4 September)

Heads of state and government in addition to other invited dignitaries expressed their views on the proposed global framework for climate services, noted the findings of the expert segment of the Conference, and, along with ministers and other national representatives, adopted a Conference Declaration calling on WMO and its partner organizations to implement the proposed framework (the Global Framework for Climate Services) without delay.

Mr. Kunio Sakurai, Director-General of JMA, said in his statement that Japan will make every effort to ensure the timely provision of climate information based on observation and research networks, and to promote their application for disaster countermeasures, water resource management, infrastructure planning and other policy measures by making the most of the knowledge and expertise gained from WCC-3 in order to contribute to the development of the framework.

(Ryuji Yamada, Tokyo Climate Center, Climate Prediction Division)



Ms. Kumi Hayashi, Head of TCC, gives a presentation on the activities of Regional Climate Centers in Asia.



Mr. Kunio Sakurai, Director-General of JMA, makes a statement at the High-level Segment.

El Niño Outlook (October 2009 – April 2010)

El Niño conditions currently prevail, and are likely to continue until boreal winter.

Pacific Ocean

In September 2009, the SST deviation from a sliding 30-year mean SST averaged over the NINO.3 region was +0.7°C. The five-month running-mean value of NINO.3 SST deviations was +0.7°C for July, and the Southern Oscillation Index for September 2009 was +0.3. In September, SSTs were above normal over the whole of the equatorial Pacific (Figures 1 and 3a), and subsurface temperature anomalies were remarkably positive from the western to the central equatorial Pacific (Figures 2 and 3b). During September, westerly wind anomalies over the western equatorial Pacific and easterly wind anomalies over the central part were found in the lower troposphere.

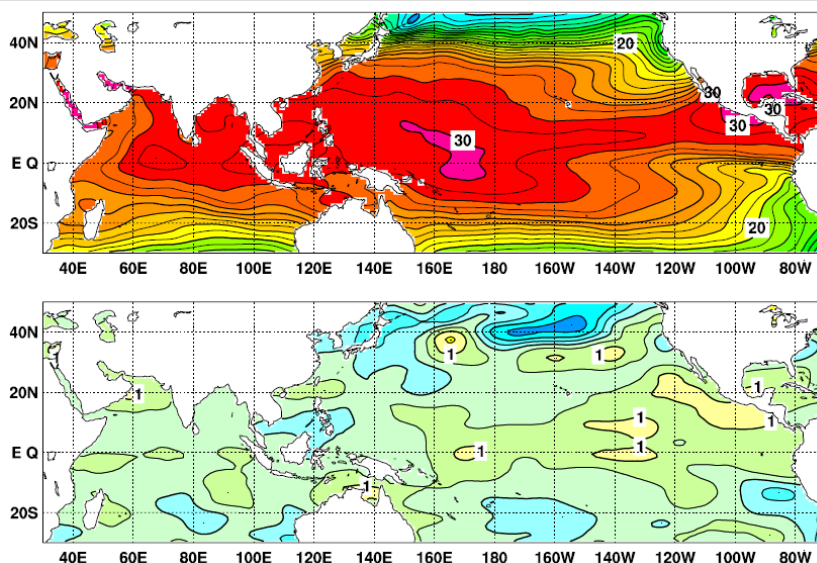


Figure 1 Monthly mean (a) sea surface temperatures (SSTs) and (b) SST anomalies in the Indian and Pacific Ocean areas in September 2009

Contour intervals are 1°C in (a) and 0.5°C in (b). The base period for the normal is 1971 – 2000.

The subsurface warm waters that had migrated from the western to the central equatorial Pacific during August were weakened by easterly wind anomalies over the central part in September. On the other hand, westerly wind anomalies prevailed over the western equatorial Pacific through September, and warm waters accumulated in western and central parts. These warm waters are expected to migrate eastward and strengthen positive SST anomalies in the eastern equatorial Pacific in the months ahead.

JMA's El Niño prediction model suggests that NINO.3 SST deviations will be above normal during the prediction period (Fig. 4).

Considering all the above factors, El Niño conditions currently prevail, and are likely to continue until boreal winter.

The SST averaged over the western tropical Pacific (NINO.WEST) region has been near normal* since boreal spring. It is likely that the SST in NINO.WEST will gradually shift to below normal in boreal autumn and winter.

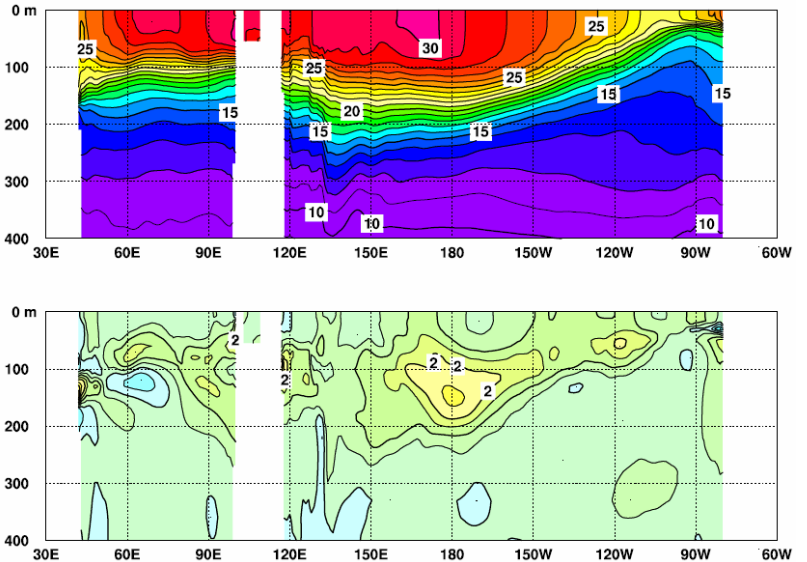


Figure 2 Monthly mean depth-longitude cross sections of (a) temperatures and (b) temperature anomalies in the equatorial Indian and Pacific Ocean areas for September 2009

Contour intervals are 1°C in (a) and 0.5°C in (b). The base period for the normal is 1979 – 2004.

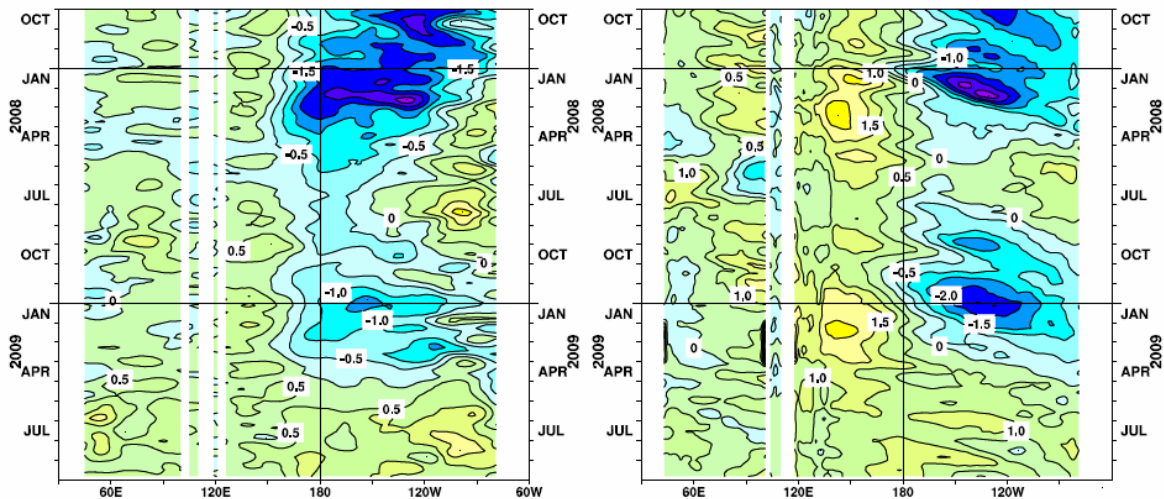


Figure 3 Time-longitude cross sections of (a) SST and (b) ocean heat content (OHC) anomalies along the equator in the Indian and Pacific Ocean areas

OHC is defined here as vertical averaged temperatures in the top 300 m. The base periods for the normals are 1971 – 2000 for (a) and 1979 – 2004 for (b).

Indian Ocean

The SST averaged over the tropical Indian Ocean (IOBW) region was slightly above normal* this summer and near normal in September. It is likely that the SST in the IOBW region will be near normal or slightly above normal during boreal autumn and winter.

Impacts on the global climate

Warmer-than-normal conditions in the northern part of South America in September were consistent with common patterns seen in past El Niño events.

(Ichiro Ishikawa, Climate Prediction Division)

* Normals for NINO.WEST (Eq. – 15°N, 130°E – 150°E) and IOBW (20°S – 20°N, 40°E – 100°E) are defined as linear extrapolations with respect to a sliding 30-year period in order to remove the effects of long-term trends.

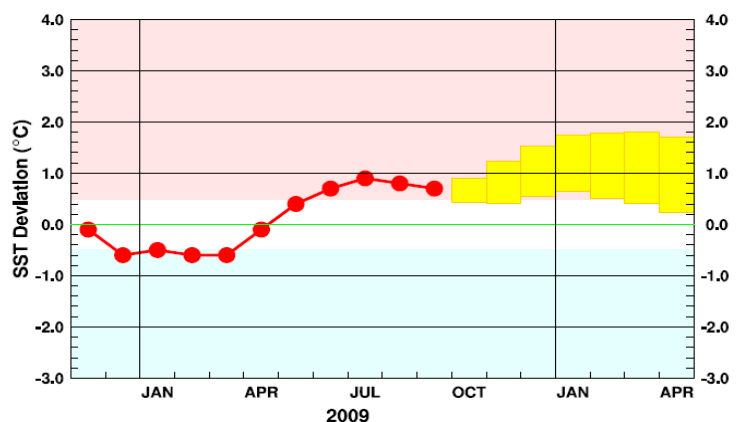


Figure 4 Outlook of SST deviation for NINO.3 produced by the El Niño prediction model

This figure shows a time series of monthly SST deviations for NINO.3 (5°N – 5°S, 150°W – 90°W). The thick line with closed circles shows observed SST deviations, and the boxes show the values produced for the next six months by the El Niño prediction model. Each box denotes the range in which the SST deviation is expected to fall with a probability of 70%.

JMA's Seasonal Numerical Ensemble Prediction for Winter 2009/2010

In winter 2009/2010, active convection is predicted from the central to the eastern tropical Pacific and the Indian Ocean, while inactive convection is predicted for the western tropical Pacific. Predicted atmospheric circulation patterns in the tropics are generally consistent with the atmospheric response associated with El Niño conditions. In the mid-high latitudes, the Aleutian Low is predicted to shift eastward and the Siberian High is expected to be weaker than normal, indicating that the winter monsoon in East Asia is likely to be weaker than normal.

1. Introduction

This report outlines JMA's seasonal numerical ensemble prediction for winter 2009/2010 (December 2009 – February 2010), which was used as a prognostic tool in the Agency's operational cold-season outlook issued on 22 October 2009. The prediction consists of 51 ensemble members with an initial date of 16 October 2009, and employs a two-tier method: first, global SSTs are predicted using a combination of persistent anomalies, climatology and forecasting using JMA's El Niño prediction model (an atmosphere-ocean coupled setup), and specific SSTs are then fed into an atmospheric model. Details of the prediction system and verification maps based on 22-year hind-cast experiments (1984 – 2005) are available at <http://ds.data.jma.go.jp/tcc/tcc/products/model/index.html>. Section 2 below presents the global SST anomalies predicted, followed in Section 3 by a description of the predicted circulation fields in the tropics and subtropics associated with these anomalies. Finally, the predicted circulation fields in the middle and high latitudes of the Northern Hemisphere are explained in Section 4.

2. SST anomalies

In September 2009, positive SST anomalies were found in most parts of the tropics. The El Niño Monitoring Index (i.e., the SST deviation from a sliding 30-year mean SST

averaged over the NINO.3 region) was above normal (+0.7), indicating the current prevalence of El Niño conditions. According to the El Niño outlook, above-normal NINO.3 SST deviations are likely to continue during winter 2009/2010.

The SST anomalies used in JMA's seasonal numerical ensemble prediction system are shown in Figure 5. It is predicted that above-normal SST anomalies will continue during winter 2009/2010 in most parts of the tropics. Large positive anomalies were found in the eastern equatorial Pacific in particular, reflecting El Niño conditions. Large positive anomalies were also found in the tropical Indian Ocean.

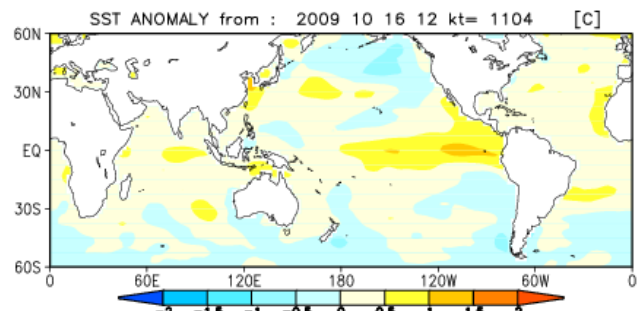


Figure 5 Predicted SST anomalies for 2009/2010 DJF

3. Circulation fields in the tropics and sub-tropics (Figure 6)

In the tropical Pacific, precipitation is predicted to be above normal from central to eastern parts, and is expected to be below normal east of the Philippines and in the western South Pacific (the area referred to as the South Pacific Convergence Zone, or SPCZ). In the Indian Ocean, precipitation is predicted to be above normal, especially from central to western parts. The values of 200-hPa velocity potential anomalies are negative (i.e., more divergent) in the Indian Ocean and positive (i.e., more convergent)

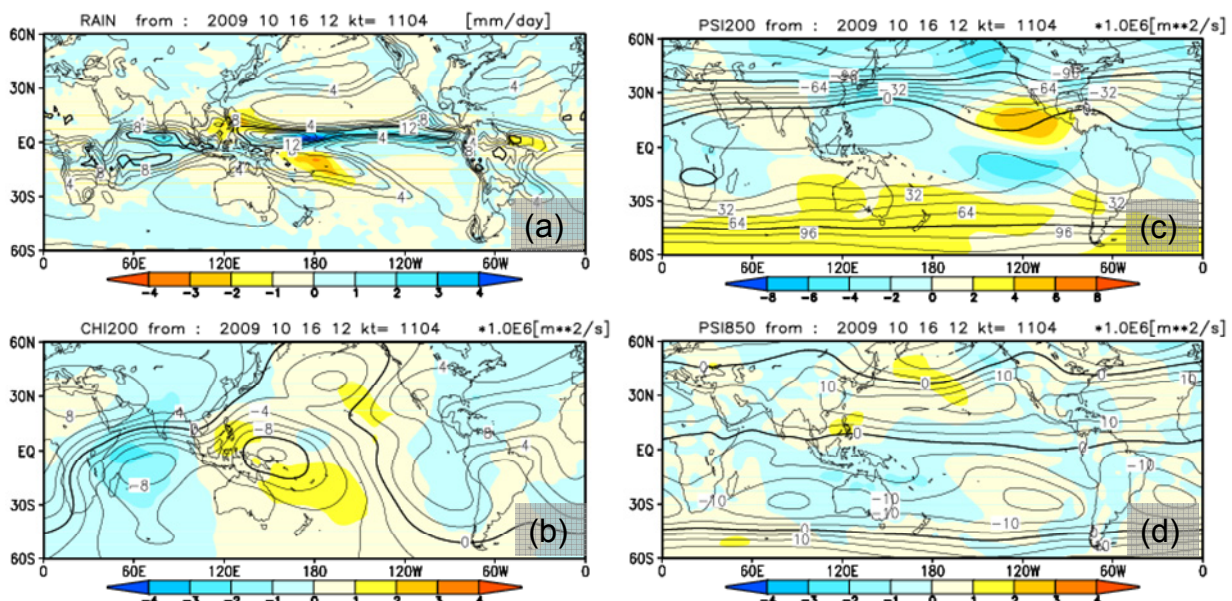


Figure 6 Predicted atmospheric fields in the tropics and sub-tropics for 2009/2010 DJF (ensemble mean of 51 members)

- (a) Precipitation (contours) and anomaly (shaded). The contour interval is 2 mm/day.
- (b) Velocity potential at 200 hPa (contours) and anomaly (shaded). The contour interval is 2×10^6 m²/s.
- (c) Stream function at 200 hPa (contours) and anomaly (shaded). The contour interval is 16×10^6 m²/s.
- (d) Stream function at 850 hPa (contours) and anomaly (shaded). The contour interval is 5×10^6 m²/s.

around the western equatorial Pacific, reflecting precipitation anomaly patterns in the tropics. Slightly negative velocity potential anomalies are found in the eastern equatorial Pacific. In the 850-hPa stream function field, equatorially symmetric anti-cyclonic and cyclonic circulation anomalies are predicted from the Indian Ocean to Southeast Asia and over the Pacific, respectively. In the 200-hPa stream function field, equatorially symmetric cyclonic and anti-cyclonic circulation anomalies are predicted over East Asia/the South Indian Ocean and in the eastern Pacific, respectively. Relatively anti-cyclonic anomalies are predicted from South Asia to the Arabian Sea, and cyclonic anomalies are predicted around East Asia, which may reflect the contrast of convective activities between the Indian Ocean and the western equatorial Pacific.

These anomaly patterns are generally consistent with the atmospheric response associated with El Niño conditions (cf. the statistical relationship between atmospheric circulation and El Niño Monitoring Index values on the TCC web page at <http://ds.data.jma.go.jp/tcc/tcc/products/clisys/newoceanindex/explanation.html>). According to the results of hindcasting, prediction skill for the atmospheric response associated with El Niño conditions is high. The characteristics of the predicted anomalies for the atmospheric circulation fields described above are therefore reliable. How-

ever, cyclonic circulation anomalies for the 200-hPa stream function over East Asia show an eastward shift in relation to the statistical relationship. This may be related to active convection in the Indian Ocean. However, considering the prediction skill for precipitation over the Indian Ocean, the reliability of the detailed distribution of such anomalies over East Asia should be treated with caution.

4. Circulation fields in the middle and high latitudes of the Northern Hemisphere (Figure 7)

In the 500-hPa height field, positive anomalies are predicted over the mid-latitudes in relation to globally warmer-than-normal SSTs. Positive anomalies in the North Pacific, negative anomalies in southern Alaska and positive anomalies in North America are predicted, forming a pattern similar to that of the Tropical Northern Hemisphere (TNH) and reflecting El Niño conditions. In the sea level pressure field, negative anomalies are predicted from the Bering Sea to the area south of Alaska, indicating that the location of the Aleutian Low is expected to shift eastward. Positive anomalies are predicted to the east of Japan, while negative values are expected over Siberia. These anomaly patterns suggest that the winter monsoon in East Asia is likely to be weak.

(Masayuki Hirai, Climate Prediction Division)

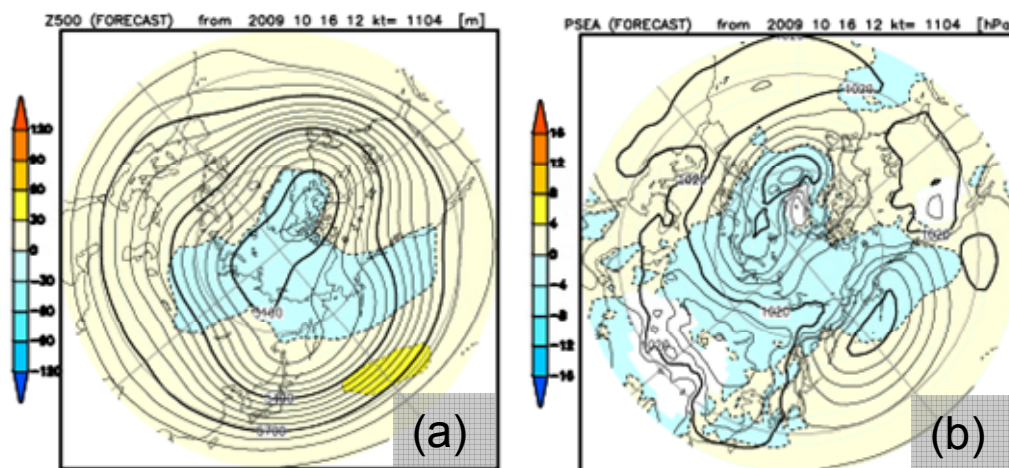


Figure 7 Predicted atmospheric fields in the middle and high latitudes of the Northern Hemisphere for 2009/2010 DJF (ensemble mean of 51 members)

(a) 500-hPa height (contours) and anomaly (shaded). The contour interval is 60 m.
 (b) Sea level pressure (contours) and anomaly (shaded). The contour interval is 4 hPa.

Cold-season Outlook for Winter 2009/2010 in Japan

JMA's seasonal forecast for winter 2009/2010, issued on 24 September 2009, indicates above-normal temperatures with 60% probability in Okinawa/Amami and 50% probability in eastern and western Japan.

1. Oceanic conditions

In August 2009, the SST deviation from a sliding 30-year mean SST averaged over the NINO.3 region was +0.8°C. The Southern Oscillation Index for August 2009 was -0.3, and SSTs for the same month were above normal for the whole of the equatorial Pacific. Subsurface temperature anomalies were remarkably positive from the western to the central equatorial Pacific. During August, westerly wind anomalies were found in the lower troposphere over the eastern equatorial Pacific, and subsurface warm waters migrated from the western to the central equatorial Pacific during the same month. These conditions indicate that

positive SST anomalies in the eastern equatorial Pacific will strengthen in the months ahead. JMA's El Niño prediction model suggests that NINO.3 SST deviations will be above normal during the prediction period.

Considering all the above factors, El Niño conditions currently prevail, and are likely to continue until the coming winter (December-January-February). Since El Niño and La Niña events are the most important for seasonal prediction and are likely to develop during winter, high reliability is expected in regard to the prediction for the coming winter season.

Considering all the above factors, El Niño conditions currently prevail, and are likely to continue until the coming winter (December-January-February). Since El Niño and La Niña events are the most important for seasonal prediction and are likely to develop during winter, high reliability is expected in regard to the prediction for the

coming winter season.

In recent years, positive SST anomalies have persisted over most of the world. From June to August 2009 in particular, global averaged monthly SST anomalies consecutively set new records for these months. As El Niño conditions are expected to continue, it is likely that the global averaged SST anomaly will continue to be above normal during the coming winter.

2. Numerical Prediction

The SST anomaly pattern fed to the atmospheric global model is very similar to that of El Niño events (i.e., below normal in the western Pacific and above normal in the central/eastern Pacific and in the Indian Ocean).

In association with the SST anomaly pattern, the predicted ensemble averaged atmospheric circulation anomaly pattern produced by the model is also very similar to that of El Niño events in the tropics and the sub-tropics as outlined below.

In the lower-tropospheric (850 hPa) stream function field, equatorially symmetric anti-cyclonic and cyclonic circulation anomalies are clearly predicted from the Indian Ocean to Indonesia extending to the south of Japan and over the Pacific, respectively (Figure 8). Anti-cyclonic circulation anomalies extending to the south of Japan suggest that warm and humid air is likely to flow to the south of the country, creating favorable conditions for the formation of cyclones.

In the upper-tropospheric (200 hPa) stream function field, equatorially symmetric cyclonic and anti-cyclonic circulation anomalies are clearly predicted over East Asia/the South Indian Ocean and from the equatorial central to eastern Pacific, respectively. In line with the cyclonic circulation anomalies over East Asia, the subtropical jet streams are predicted to shift southward over China and northward over Japan, suggesting weak winter monsoon activity around Japan.

According to the results of hindcasting (covering the 22 years from 1984 to 2005), prediction skill for anomaly patterns associated with El Niño conditions (Figure 9) is high. In the mid- and high latitudes, a neutral phase of Arctic Oscillation (AO) is predicted. The positive (negative) phase of AO tends to cause a weak (strong) winter monsoon and above-normal (below-normal) temperatures in northern Japan. However, the spread among ensemble members is large, and hindcasting suggests that the model does not have a sufficient level of skill to predict AO.

3. Long-term trend and decadal variation

Long-term upward trends are clearly seen in winter mean temperatures over Japan except in the northern part of the country. In northern Japan, winter mean temperatures show large year-to-year fluctuations, while the winter mean temperature for the last ten years has been near normal,

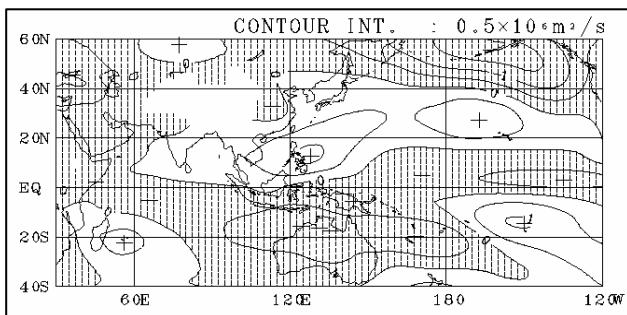


Figure 9 Composite of 850-hPa stream function anomaly for El Niño events in boreal winter (contour interval: $0.5 \times 10^6 \text{ m}^2/\text{s}$) Light, medium and heavy shading shows confidence levels of 90%, 95% and 99% respectively based on t-testing.

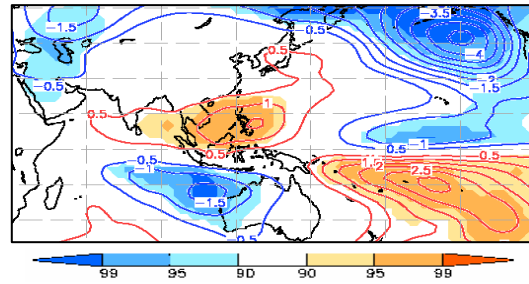


Figure 8 Predicted 850-hPa stream function anomaly for winter 2009/2010 The contour interval is $0.5 \times 10^6 \text{ m}^2/\text{s}$.

partly affected by the weak negative phase of AO decadal oscillation. Winter precipitation has tended to be above normal on the Pacific side of northern, eastern and western Japan since the end of the 1990s.

The tropospheric thickness temperature averaged over the mid-latitudes of the Northern Hemisphere ($30^\circ\text{N} - 50^\circ\text{N}$), which shows a positive correlation with temperatures in Japan, has tended to be above normal since 2006, and is predicted to continue to be above normal because of the positive global SST anomaly.

4. Conclusion

Numerical prediction indicates that above-normal temperatures will prevail in winter over the whole of Japan in response to the prevailing El Niño conditions. However, considering the prediction skill for AO and the long-term trend, it is likely that temperatures in northern Japan will be lower than the results of this numerical prediction suggest. In regard to precipitation, favorable conditions for the formation of cyclones over the south of Japan are expected to bring above-normal precipitation on the Pacific side and in the southern part of the country.

5. Outlook summary

JMA's cold season outlook predicts above-normal temperatures with 60% probability in Okinawa/Amami and 50% probability in eastern and western Japan (Figure 10). It also indicates both near-normal and above-normal precipitation levels with 40% probability on the Pacific side of eastern and western Japan and in Okinawa/Amami. The outlook for cold season snowfall on the Sea of Japan side of the country calls for below-normal amounts with 50% probability in eastern and western Japan, and both near-normal and below-normal amounts with 40% probability in northern Japan.

(Hiroshi Nakamigawa, Climate Prediction Division)

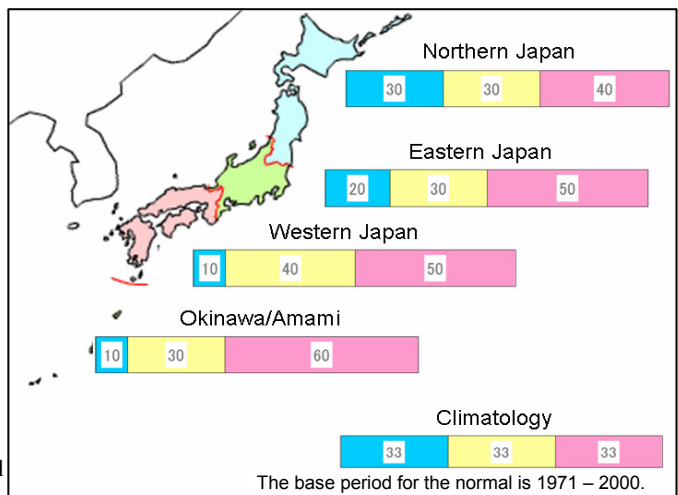


Figure 10 Outlook for winter 2009/2010 temperature probability in Japan The base period for the normal is 1971 – 2000.

Summary of the 2009 Asian Summer Monsoon

1. Monsoon activities and atmospheric circulation

Asian summer monsoon activity inferred from the seasonal mean (i.e., from June to September) of Outgoing Longwave Radiation (OLR) was enhanced from the area east of the Philippines to the western Pacific (Figure 11), and was suppressed over western Indonesia and from India to the area around Taiwan.

Asian summer monsoon activity was generally suppressed throughout the season except in the West North Pacific Monsoon (WNPM) region. In the lower troposphere, monsoon circulation was stronger than normal over the eastern Indian Ocean, although its northward penetration was weaker than normal (Figure 12a). Cyclonic circulation anomalies were observed around the Philippines, indicating that the monsoon trough was stronger than normal. In the upper troposphere, the Tibetan High shifted southward from its normal position from the Arabian Peninsula to India in line with suppressed convection over India (Figure 12b).

Propagation of the active phase of the Madden-Julian Oscillation (MJO) tended to be obscure throughout the season. Although the active phase propagated from the Pacific to the Atlantic and the Indian Ocean from June to July, its

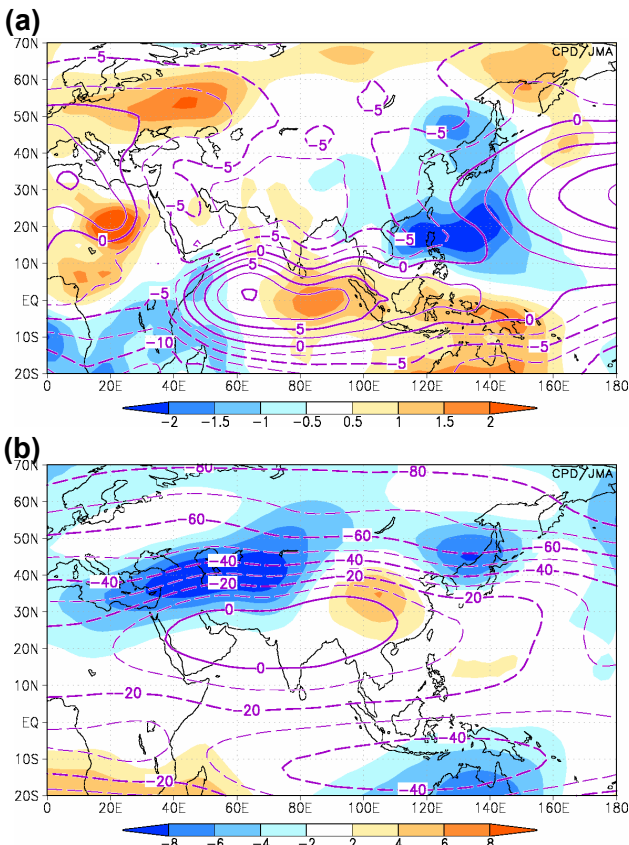


Figure 12 Four-month mean stream function and its anomaly for June – September 2009

(a) Contours indicate 850-hPa stream function (m^2/s) at intervals of $2.5 \times 10^6 \text{ m}^2/\text{s}$, and color shading indicates 850-hPa stream function anomalies. (b) Contours indicate 200-hPa stream function (m^2/s) at intervals of $10 \times 10^6 \text{ m}^2/\text{s}$, and color shading indicates 200-hPa stream function anomalies.

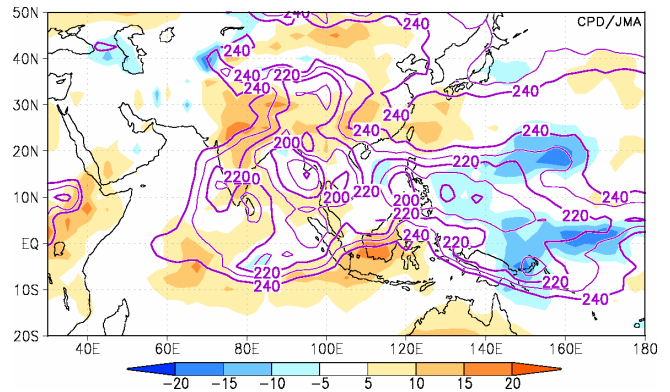


Figure 11 Four-month mean OLR and its anomaly for June – September 2009

Solid lines indicate OLR (W/m^2) with a contour interval of $10 \text{ W}/\text{m}^2$, and color shading indicates OLR anomalies.

propagation became obscure thereafter. Around India, northward propagation of active convection was rarely observed, corresponding to the delay in the onset of the monsoon in India. Remarkable monsoon breaks were observed three times in India (Figure 13a), and northward propagation of active convection was observed in early June, early August and early September over the area east of the Philippines. In the western Pacific, convective activity was extremely enhanced in July. Variations over periods of about 30 days dominated the WNPM region throughout the season (Figure 13b).

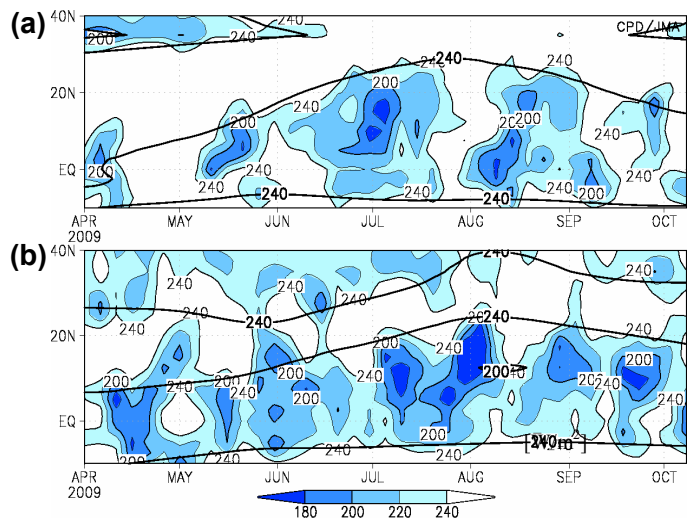


Figure 13 Latitude-time cross section of the five-day mean OLR from April to October 2009 ((a) India (65 – 85°E mean), (b) area east of the Philippines (125 – 145°E mean))

Thick black lines indicate the climatological mean OLR for the period from 1979 to 2004. Shading indicates the OLR in 2009 (W/m^2).

2. Precipitation, temperature and extreme events

Total precipitation amounts based on CLIMAT reports during the monsoon season (June – September) were below normal in most areas from eastern to southern Asia, and in particular were below 60% of the normal in northern India and southern Mongolia (Figure 14). Amounts were mostly consistent with the distribution of OLR anomalies (Figure 11), but were above 120% of the normal around the northern part of the Sea of Japan and in some parts of western India.

Four-month mean temperatures for the same period were higher than normal over most parts of eastern to southern Asia except around northeastern and northwestern China (Figure 15).

Extremely heavy precipitation was observed around the northern part of the Sea of Japan in June and around the Sea of Japan in July. In contrast, extremely light precipitation was observed around western Mongolia in June, from eastern Siberia to eastern Mongolia in July, and from northern Japan to southern China in September (figures not shown).

On the other hand, monthly mean temperatures were extremely high in many regions throughout the season, especially in low latitudes south of 30°N.

In the area of monsoon activity, total fatalities during the season were reported to be more than 1,100 in India. Drought damage was also reported in India and Bangladesh. In Japan, Baiu front activity caused 31 fatalities in late July. In China, heavy rains and storms caused damage from June to August.

Table 1 Tropical cyclones forming in the western North Pacific from June to September 2009

ID number	Name	Date (UTC)	Category ¹⁾	Maximum wind speed ²⁾ (knots)
T0903	Linfa	6/18 – 6/22	STS	60
T0904	Nnagka	6/23 – 6/26	TS	40
T0905	Soudelor	7/11	TS	35
T0906	Molave	7/16 – 7/19	TY	65
T0907	Goni	8/3 – 8/8	TS	40
T0908	Morakot	8/3 – 8/10	TY	75
T0909	Etau	8/9 – 8/12	TS	40
T0910	Vamco	8/17 – 8/25	TY	90
T0911	Krovanh	8/28 – 9/1	STS	85
T0912	Dujuan	9/3 – 9/9	STS	70
T0913	Mujigae	9/10 – 9/11	TS	35
T0914	Choi-wan	9/12 – 9/20	TY	100
T0915	Koppu	9/13 – 9/15	TY	65
T0916	Ketsana	9/26 – 9/30	TY	105
T0917	Parma	9/29 – 10/14	TY	150
T0918	Melor	9/29 – 10/9	TY	110

Note: Tentatively prepared by the RSMC Typhoon Center

1) Intensity classification of tropical cyclones

TS: Tropical Storm

STS: Severe Tropical Storm

TY: Typhoon

2) Estimated maximum 10-minute mean winds

3. Tropical cyclones (TCs)

During the monsoon season, 16 TCs of tropical storm (TS) intensity or higher formed in the western North Pacific and the South China Sea (Figure 14 and Table 1). The number of formations was almost the same as the 1971 – 2000 average of 16.4. Nine TCs moved over the South China Sea and approached southern China or Vietnam. In particular, Typhoon Parma, which formed in late September, moved westward and hit the Philippines in early October. In the western North Pacific, four TCs moved north-eastward over the south of Japan's main islands.

In the Philippines, TCs Nangka, Molave, Morakot and Ketsana caused more than 500 fatalities in total, and Typhoon Parma caused more than 460 fatalities in early October. Typhoon Morakot also caused 8 fatalities in China, and Typhoon Ketsana caused more than 160 fatalities in Vietnam. In August, Severe Tropical Storm Etau caused 25 fatalities in Japan. In September, Typhoon Koppu caused 7 fatalities in China.

Note: Disaster information is based on reports by governmental organizations (China, India, Japan and the Philippines) and UN organizations (IRIN and OCHA-Kobe)

(1. Hiroshi Hasegawa, 2 – 3. Yoshikazu Fukuda, Climate Prediction Division)

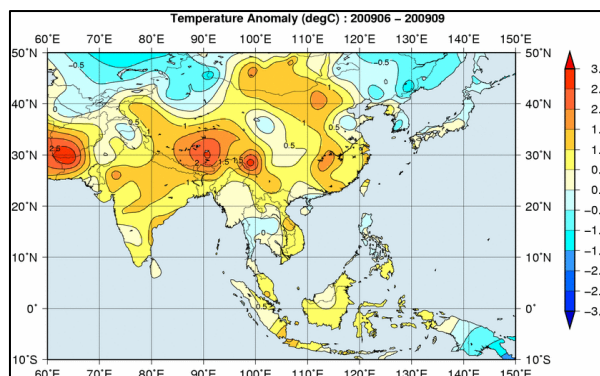


Figure 14 Four-month precipitation ratio (%) and tropical cyclone tracks in the northwestern Pacific from June to September 2009

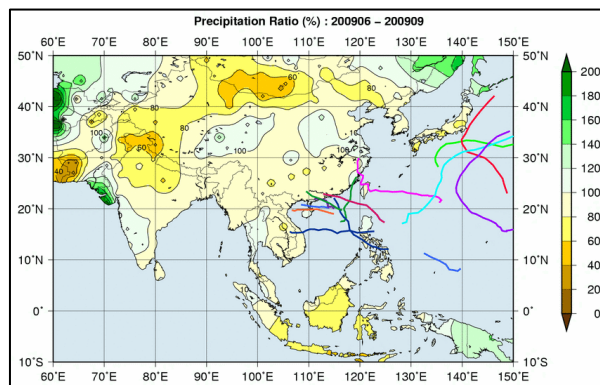


Figure 15 Four-month mean temperature anomaly (°C) from June to September 2009

Status of the Antarctic Ozone Hole in 2009

The Antarctic ozone hole in 2009 was slightly smaller than its average size over the last ten years.

In the last 30 years, the Antarctic ozone hole has appeared from late winter to early spring (August – December), with depletion peaking in September or early October. The Antarctic ozone hole is defined as the area where the total ozone column is equal to or less than 220 m atm-cm.

According to JMA's analysis of satellite data supplied by the National Aeronautics and Space Administration (NASA), the ozone hole in 2009 first appeared in mid-August and expanded rapidly in late August until it reached a maximum area of 24.0 million km² on 17 September – 1.7

times as large as the Antarctic Continent (Figure 16). It was slightly smaller than its average size of 26.2 million km² seen over the last ten years, and was the 15th largest since 1979. The five spheres at the bottom of Figure 16 show total ozone distributions in the Southern Hemisphere with the ozone hole shown in gray.

The Antarctic ozone hole is expected to continue for decades according to *WMO/UNEP Scientific Assessment of Ozone Depletion: 2006*. Close observation of the status of the ozone layer, including the Antarctic ozone hole, remains important.

(Seiji Miyauchi, Ozone Layer Monitoring Office, Atmospheric Environment Division)

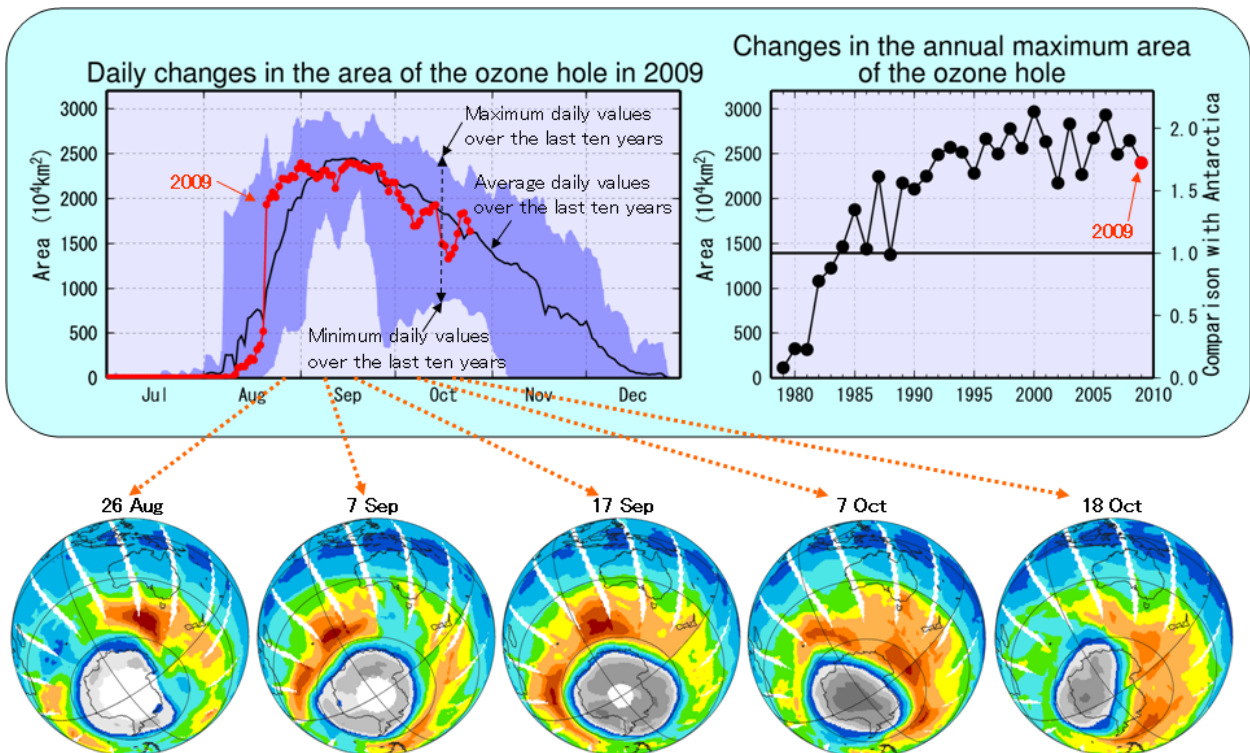


Figure 16 Daily changes in the area of the ozone hole in 2009 (left) and changes in its annual maximum area since 1979 (right), and total ozone distributions in the Southern Hemisphere on the indicated dates (bottom)

The Antarctic ozone hole is shown in gray with white areas indicating missing data. These figures and distributions were produced from TOMS and OMI data supplied by NASA.

Heavy precipitation in the Philippines and India from late September to early October 2009

Weather conditions and damage

Typhoon Ketsana moved slowly westward from Luzon Island in the Philippines to Vietnam in late September (Figure 17), and heavy precipitation was observed around the south of Luzon Island (Figure 19). According to the Philippine Atmospheric, Geophysical and Astronomical Services Administration (PAGASA), the 410.6 mm of precipitation within nine hours recorded in Metro Manila was the capital's largest rainfall since 7 June 1967 (a 42-year period). It was reported that the resultant flood disaster caused more than 460 fatalities (National Disaster Coordinating Council of the Philippines: NDCC).

Typhoon Parma moved around northern Luzon Island very slowly (Figure 18), and caused heavy precipitation there in early October (Figure 20). Nine days of rainfall from 1 to 9

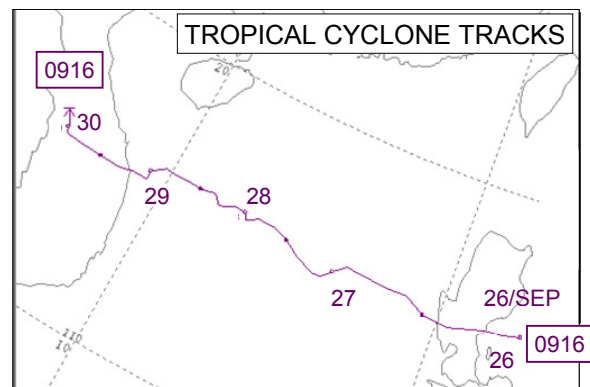


Figure 17 Track of Typhoon Ketsana (26 – 30 September 2009)

October amounted to more than 1,870 mm of precipitation (around 1,160% of the normal) in Baguio City. It was reported that the heavy precipitation caused more than 460 fatalities (NDCC).

Meanwhile, a low-pressure area that formed on 28 September became well marked the following day, and remained around the western central Bay of Bengal until early October. Heavy precipitation was observed in southern India, and six days of rainfall from 28 September to 3 October produced 309 mm of precipitation in Kurnool (around 1,290% of the normal) and 407 mm in Honavar (around 1,040% of the normal) (Figure 21). It was reported that the heavy precipitation caused more than 320 fatalities in India (Indian Ministry of Home Affairs).

(Takafumi Umeda, Climate Prediction Division)

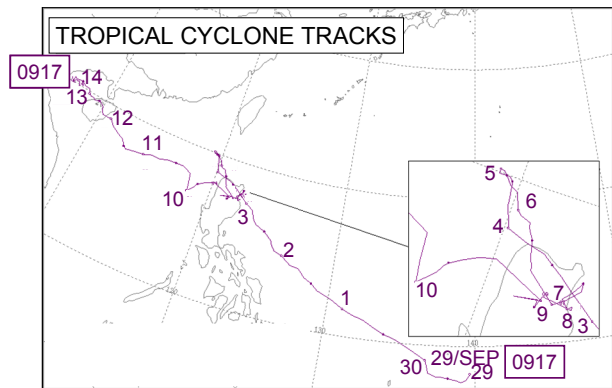


Figure 18 Track of Typhoon Parma (29 September – 14 October 2009)

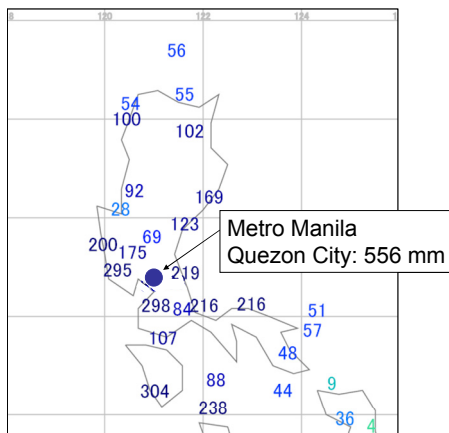


Figure 19 Six-day precipitation amount around Luzon Island (25 – 30 September 2009, unit: mm)

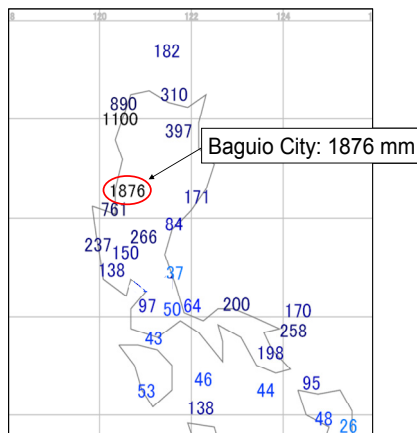


Figure 20 Nine-day precipitation amount around Luzon Island (1 – 9 October 2009, unit: mm)

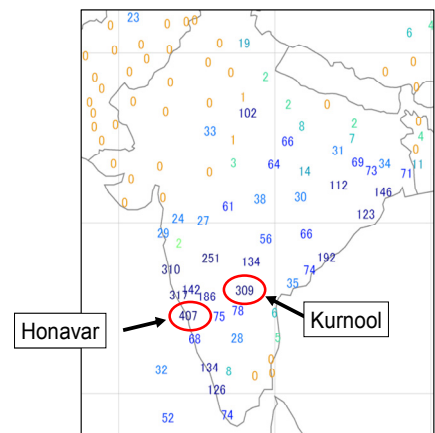


Figure 21 Six-day precipitation amount in India (28 September – 3 October 2009, unit: mm)

Conditions of convective activity and atmospheric circulation

Strong convective activity persisted in the equatorial western Pacific throughout September 2009. It became extremely enhanced in the second half of the month (blue shading in Figure 22), causing remarkable development of an equatorial Rossby wave (upper panel of Figure 22). Cyclonic circulation anomalies (the red oval in the upper panel of Figure 22) corresponded to the development of this equatorial Rossby wave, which took on a spatial scale of about 5,000 km. In late September, the westward propagation of the equatorial Rossby wave was clear (the red arrows in Figure 22). Moreover, smaller-scale and remarkable cyclonic circulation anomalies formed over the northern part of the South China Sea (the red “C” in the lower panel of Figure 22), indicating the development of Typhoon Ketsana. In addition, Typhoon Parma developed in the region of the westward propagation of the equatorial Rossby wave afterwards. At the end of September, this equatorial Rossby wave finally reached India and enhanced convective activity in the region (lower panel of Figure 22).

(Yayoi Harada, Climate Prediction Division)

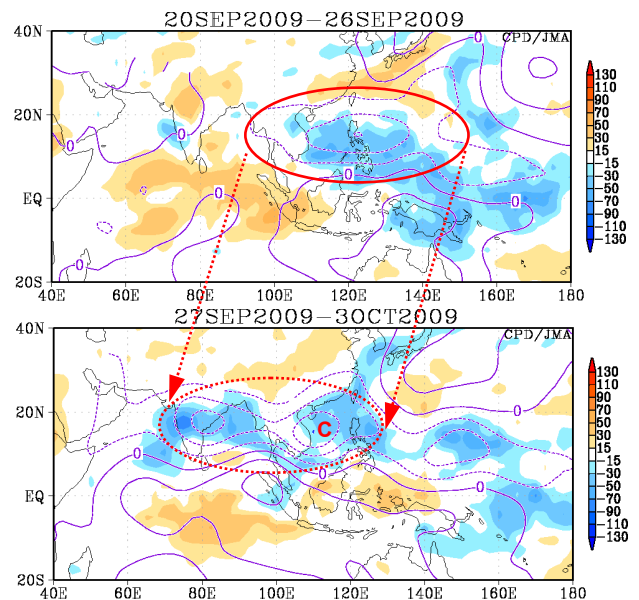


Figure 22 Seven-day mean OLR anomalies (shading) and 850-hPa stream function anomalies (contours)
Shading shows OLR anomalies in units of $W m^{-2}$. Contours show 850-hPa stream function anomalies at intervals of $2.5 \times 10^6 m^2 s^{-1}$. Upper panel: 20 – 26 September 2009; Lower panel: 27 September – 3 October 2009.

Any comments or inquiries on this newsletter and/or the TCC website would be much appreciated. Please e-mail to: tcc@climar.kishou.go.jp

(Chief Editor: Kumi Hayashi)

Tokyo Climate Center (TCC), Climate Prediction Division, JMA
Address: 1-3-4 Otemachi, Chiyoda-ku, Tokyo 100-8122, Japan
TCC website: <http://ds.data.jma.go.jp/tcc/tcc/index.html>